Arabian Journal of Chemistry (2022) **15**, 104285

King Saud University

Arabian Journal of Chemistry

www.ksu.edu.sa
www.sciencedirect.com

ORIGINAL ARTICLE

Influence of different parameters on the rheological behavior MWCNT (30%)-TiO_2 (70%) / SAE50 hybrid nano-lubricant using of response surface methodology and artificial neural network methods

Mohammad Hemmat Esfe [a], Mahmoud Kiannejad Amiri [b], Saeed Esfandeh [a], Mohammad Reza Sarmasti Emami [b], Davood Toghraie [c,*]

[a] *Department of Mechanical Engineering, Imam Hossein University, Tehran, Iran*
[b] *University of Science and Technology of Mazandaran, Mazandaran, Iran*
[c] *Department of mechanical engineering, Khomeinishahr branch, Islamic Azad University, Khomeinishahr, Iran*

Received 29 October 2021; accepted 18 September 2022
Available online 22 September 2022

KEYWORDS

Nanolubricant;
Viscosity;
Multi-layer Perceptron;
Response Surface Methodology;
Artificial Neural Network;
MWCNT

Abstract In this study, the effects of different parameters as the volume fraction of nanoparticles (φ), temperature, and shear rate ($\dot{\gamma}$) on viscosity (μ_{nf}) of MWCNT (30 %)-TiO_2 (70 %)/SAE50 hybrid nano-lubricant were investigated. The temperature is the most effective parameter while $\dot{\gamma}$ has less influence on μ_{nf}. RSM and ANN methods are used for the prediction of MWCNT (30 %)-TiO_2 (70 %)/SAE50 hybrid nano-lubricant. Results reveal that a network with 2 hidden layers with 5 neurons and a logistic sigmoid transfer function for the first layer, and 2 neurons with a tangent sigmoid transfer function for the second layer has a minimum error and maximum efficiency. Also, using statistical regression analysis considering training and test data (R = 0.9999) and comparison of ANN estimated values with empirical data have shown the good capability of μ_{nf} prediction by improved ANNs (Mean square error of 1.3367 and mean absolute error of 0.7663). By comparing the two presented models, it was found that the ANN model can predict the viscosity of the investigated nanofluid better than the RSM model.

* Corresponding author.
E-mail addresses: m.hemmatesfeh@gmail.com (M. Hemmat Esfe), Toghraee@iaukhsh.ac.ir (D. Toghraie).

Peer review under responsibility of King Saud University.

Production and hosting by Elsevier

https://doi.org/10.1016/j.arabjc.2022.104285
1878-5352

Nomenclature

ANN	Artificial Neural Network
MLP	Multilayer Perceptron
d	grain size of the particle
FCM-ANFIS	Fuzzy C Means-Adaptive Neuro Fuzzy Inference System
FWHM	Full width at half maximum
y_i	difference of considerations
$\widehat{y}_i$	fitted values
MAE	mean absolute error
MOD	margins of deviation
MSE	mean square error
MWCNT	Multi-walled carbon nanotube
TiO_2	Titanium dioxide
CuO	Copper oxide
Al_2O_3	Aluminum oxide
SiO_2	Silicon dioxide
MgO	Magnesium oxide
SAE	Society of Automotive Engineers
SVF	Solid volume fraction
SS_E	Sum of squares of residuals
SSA	Specific Surface Area
y_i	difference of considerations
$\widehat{y}_i$	fitted values
S_T	Total sum of squares
R^2	determination coefficient
n	Number of measurement
RSM	Response Surface Methodology
XRD	X-ray Diffraction

Greek symbols

μ_{nf}	Dynamic viscosity of nanofluid (mPa.*sec*)
φ	Volume fraction of nanoparticles
λ	wavelength (Å)
θ	Bragg angle
τ_{yx}	Shear stress (Pa)
$\dot{\gamma}$	Shear rate (s^{-1})
ρ	Density
γ_{jk}	the output of j neuron from k layer
β_{jk}	weight for j neuron in k layer

Subscripts

bf	base fluid
nf	nanofluid
p	particles
n	power law index
B	highest peak
C	crystal factor uncertainty
d	diameter of particles (nm)
m	consistency index
T	Temperature
W	Weight

1. Introduction

In recent decades, the role of nanotechnology in the development of engineering sciences has been significant and abundant, and there have always been many and interesting researches on various branches of nanotechnology (Zhang et al., 2015; Zhang et al., 2015; Gao et al., 2019; Dwijendra et al., 2022; Kazemi and Shiri, 2022; Gupta, 2022; Rakshe et al., 2021; Azin and Pourghobadi, 2021; Asif, 2018; Athab et al., 2015). Also, fluids, as a main component in various branches of engineering sciences, perform many applications in the field of lubrication, heat transfer, fluid transfer, etc., and research on various fluid parameters has always been one of the most important engineering challenges (Wang et al., 2016; Zhang et al., 2022; Zhang et al., 2022; Li and Zhao, 2022). In recent decades, nanoparticles play important role in all branches of sciences (Yang et al., 2017; Desai et al., 2021; Mohammed et al., n.d.). Nanofluids are prepared by dispersing the particles (oxide ceramics, polymers, glass-ceramics, nitrides metals non-metals, etc.) in nano sizes and diameters < 100 nm in the base fluids including water, ethylene glycol, and oil (Hemmat Esfe et al., 2017; Alirezaie et al., 2018; Hemmat Esfe et al., 2018; Ghorabaee et al., 2019; Hemmat Esfe et al., 2017; Esfe et al., 2019; Doust et al., 2015; Esfe and Motallebi, 2019; Esfe et al., 2019; Abbasian Arani et al., 2016; Hemmat Esfe et al., 2018; Ahmadi et al., 2019; Mahian et al., 2019; Mahian et al., 2019; Hemmat Esfe et al., 2017; Rostamian et al., 2017; Alirezaie et al., 2017; Hemmat Esfe et al., 2018; Kherbeet et al., 2015). Some of the main applications of nanofluids in the industry are heat exchangers, engine coolants, electronic devices, nuclear plants, and oil recovery due to the amazing properties of these kinds of fluids (Esfe et al., 2018; Hemmat Esfe and Abbasian Arani, 2018; Esfe et al., 2019; Dastmalchi et al., 2015; Esfe et al., 2018; Abbasian Arani et al., 2012; Hemmat and Davoodi, 2019; Abbasian Arani et al., 2017; Gharibshahi et al., 2018; Abbasian Arani et al., 2014; Hemmat Esfe et al., 2017; Hemmat Esfe et al., 2017; Hemmat Esfe et al., 2017; Hemmat Esfe et al., 2017; Mansoury et al., 2019). So, it is important to identify their characteristics. One of these characteristics is μ_{nf} that plays an essential role in its application in chemical and oil engineering. Viscosity is an effective parameter in fluid lubrication, pumping, heat transfer and enhanced oil recovery (Esfe et al., 2019; Ghasemi and Karimipourm, 2018; Hemmat Esfe, 2018; Hemmat Esfe et al., 2017; Hemmat Esfe and Esfandeh, 2018; Hemmati-Sarapardeh et al., 2018; Lebon and Hatim, 2018; Ruhani et al., 2019a,b; Esfe, 2015). Lots of studies were carried out on the effect of φ, temperature, nanoparticle size, nanoparticles types and base oils on μ_{nf} (Aghaei et al., 2018; Hemmat Esfe et al., 2015; Hemmat Esfe et al., 2016; Hemmat Esfe et al., 2017; Hemmat Esfe et al., 2017; Abdul Hamid et al., 2018; Gholami et al., 2018). The best way of investigating $\mu_{nf}$is conducting different experiments and measurements with special apparatus, but this method is expensive and time-consuming. Since the equipment is not calibrated and is worn out, there might be some errors. For this reason, scientists are interested in predicting μ_{nf}using theoretical and empirical correlations. All the proposed models have their limitations. Some of them are only used for spherical nanoparticles, and the application of most of them is limited by the temperature range (Esfe, ,2017; Izadi et al., 2018; Hemmat Esfe et al., 2018; Asadi and Asadi, 2016; Esfe, ,2017; Asadi et al., 2016). Another way for saving time and reducing the cost of experiments is using prediction tools like ANN for predicting the thermophysical properties of thermal systems working with nanofluids. ANN method was designed in the 1980 s, inspired by the human brain, and nowadays is applied in modeling and simulation of processes (Huai et al., 2021; Tian, 2021). Neurons are an important part of an ANN. Lots of researchers have worked on modeling properties of nanofluids (Zaferani et al., 2019; Hemmat Esfe et al., 2017; Esfe et al., 2016; Hemmat Esfe et al., 2017; Hemmat Esfe et al., 2018; Esfe et al., 2019; Hemmat Esfe et al., 2018; Esfe et al., 2018). Maharabi et al. (Mehrabi et al., 2013) presented a model for the prediction of μ_{nf} em-

ploying an adaptive neuro-fuzzy inference system (FCM-ANFIS) based on FCM and a group of experimental data. They have chosen effective μ_{nf} as the goal parameter size of nanoparticle and temperature and φ as input variables. They compared predicted viscosities with experimental data for four different nanofluids of CuO, Al_2O_3, SiO_2, and TiO_2 and in which water was used as the base fluid. Results obtained from the proposed FCM-ANFIS model fit the measured data very well. Hemmat Esfe Research Group is one of the leading groups in nanofluid studies (Esfe et al., 2015; Esfe et al., 2015; Esfe et al., 2015). They have done many studies on various nanoparticle compounds, especially in the field of hybrid nanofluids. They opened new perspectives in the optimization of nanofluids attributes and also were able to control the unwanted increase in μ_{nf} after expanding NPs in BF (Esfe et al., 2018). The rheological behavior of MWCNT-MgO in oil base nano-lubricants was investigated by Alirezaei et al. (Alirezaie et al., 2016) at various $\dot{\gamma}$; φ and temperatures. They carried out their experiments at φ = 0.0625–1 %, T = 25–50 ℃ and $\dot{\gamma}$ = 670–8700 s^{-1}, and found out that μ_{nf} falling with raising the temperature. In addition, the nanofluid shows slightly non-Newtonian behavior, but at higher temperatures, its behavior was Newtonian. So, μ_{nf} increases with increasing φ. Changing $\dot{\gamma}$ between 666.5 and 8664.5 s^{-1} caused an increase (grow to 10 %) in μ_{nf}. But increasing the temperature from T = 25 to 50 ℃ decreases the μ_{nf} about 75 %. An equation with three variables was presented to evaluate the experimental data; experimental results were also modeled with ANN. Toghraie et al. (Toghraie et al., 2019) predicted the dynamic viscosity of Ag/Ethylene glycol nanofluid in different temperatures (25–50 °C) with v φ = 0.2 %–2% by ANN. They modeled an ANN by using 6 to 31 neurons, and simulated 30 times for each neuron. The model they presented has the accuracy parameters of MSE and SSE with values of 6.9456E −5 and 0.0030, respectively. In another study, Maddah et al. (Maddah et al., 2018) explored and anticipated the relative viscosity of MWCNT/carbon (60/40)/SAE 10 W40/SAE 85 W90 (50/50) at various temperatures (25–50 °C) and φ = 0–1 % by applying ANNs based on experimental data. The Levenberg–Marquardt (LM) training algorithm was applied for updating ANN weights. The mean square error, correlation coefficient and standard deviation were equal to 2.0193E-008, 1 and 0.00021082, respectively. Also, Ahmadi et al. (Ahmadi et al., 2019) proposed three algorithms including multivariable polynomial regression (MPR), ANN–multilayer perceptron (ANN-MLP) and multivariate adaptive regression splines (MARS) are applied to model the dynamic viscosity of silver (Ag)/water nanofluid. The R^2 values for the concentrated models are 0.9998, 0.9997 and 0.9996 for the ANN-MLP, MARS and MPR algorithms, respectively. Also, the prediction of some properties of nanofluids using different algorithms by other researchers is presented in Table 1.

Based on the above literature survey, adequate tools for predicting the thermophysical properties are not available due to presented existing limitations. In addition, obvious and sufficient limitations for a correlation do not exist. For having a correlation that has an obvious condition with any limitation, a correlation based on the ANN method using RSM is proposed. Used data in referred correlation were measured by the present investigator, and for this reason, their limitations are considered in the proposed correlation. In this research, $\boldsymbol{\mu_{nf}}$ of MWCNT (30 %)-TiO_2 (70 %)/SAE50 hybrid nano-lubricant was first measured experimentally. Then by using RSM and ANN methods, the parameters affecting the $\boldsymbol{\mu_{nf}}$ were investigated and the $\boldsymbol{\mu_{nf}}$ was modeled. Obtained results from the proposed correlation of ANN were evaluated. A summary of the investigation on μ_{nf} that was used from the ANN method is presented in Table 2.

2. Experimentation

MWCNT-TiO_2 / SAE50 hybrid nano-lubricant samples were prepared with SVFs of (30:70) in SAE50 base oil with φ = 0.0625 %, 0.125 %, 0.25 %, 0.5 %, 0.75 % and 1 %. For the preparation of nano-lubricant samples, nanoparticles were purchased from Kimia Nano Danesh Company in Iran (Specifications of nanoparticles are presented in Table 3).

Then, Eq. (1) was used for the calculation of φ. Nanoparticles were then dispersed in SAE50 base oil using a two-step method,

$$\varphi\,(\%) = \frac{\left[\frac{W_{MWCNT}}{\rho_{MWCNT}}\right] + \left[\frac{W_{TiO_2}}{\rho_{TiO_2}}\right]}{\left[\frac{W_{MWCNT}}{\rho_{MWCNT}}\right] + \left[\frac{W_{TiO_2}}{\rho_{TiO_2}}\right] + \left[\frac{W_{SAE50}}{\rho_{SAE50}}\right]} \times 100 \tag{1}$$

X-ray diffraction patterns of carbon nanotubes and TiO_2 nanoparticles are shown in Fig. 1. This spectrometer shows the range of particle sizes. Morphological properties of nanoparticles were studied using X-ray diffraction and are shown in Fig. 1. The average size of TiO_2 is calculated using XRD images and the Debye-Scherrer equation (Holzwarth and Gibson, 2011);

Table 1 A summary of the research done with the prediction of some properties of nanofluids.

Reference No.	Nanofluid	Target	Algorithm	Accuracy
[96]	Al_2O_3/10 W40	relative viscosity	Levenberg–Marquardt	R = 0.995838 MSE = 4.14469E-08
(Tian et al., 2021)	Graphene oxide-Al_2O_3/ Water-Ethylene glycol	thermal conductivity	trainbr	R = 0.999 MSE = 1.67E-6
(Esfe and Motallebi, 2021)	MWCNT (10 %)-SiO_2 (90 %)/SAE50	viscosity	Levenberg–Marquardt	R = 0.9999
(Esfe et al., 2022)	MWCNT-CuO (30:70)/ SAE 50	viscosity	trainlm	R^2 = 0.9999 MSE = 0.003756
(Abu-Hamdeh et al., 2021)	MWCNT-liquid paraffin	viscosity	not mentioned	R^2 = 0.988 MSE = 0.52
(Chu et al., 2021)	MWCNT-TiO_2/5W40	relative viscosity	not mentioned	R^2 = 0.988 MSE = 0.00238
(Mirsaeidi and Yousefi, 2021)	water–ethylene glycol mixture (60:40 vol%)-based carbon quantum dots	Viscosity thermal conductivity density	not mentioned	AAD = 1.29 % R^2 = 0.99994 AAD = 0.85 % R^2 = 0.99867 AAD = 0.01 % R^2 = 0.99999

Table 2 Summary of the research work done on oil with nanofluids.

Reference No.	Condition	Results
(Hemmat Esfe and Tilebon, 2019)	ϕ = 0–1.5 %; T = 25–50 °C	Optimum viscosity and heat conduction were reported in maximum operating temperature
(Aghahadi et al., 2019)	ϕ = 0.05–0.6 %; T = 20–60 °C	Newtonian behavior
(Asadi et al., 2018)	T = 20–55 °C	Highly efficient in heat transfer application as a coolant fluid
(Alarifi et al., 2019)	ϕ = 0.0025–0.02; T = 25–50 °C	Newtonian behavior
(Wei et al., 2017)	φ = 0–0.01; T = 15–45 ^{O}C	Newtonian behavior
(Gulzar et al., 2019)	ϕ = 0.005–0.05; T = 20–150 °C	Newtonian behavior
(Liu et al., 2018)	ϕ = 0.01–0.04; T = 20 °C	$\mu_{nf}$of hybrid nanofluid is lower than a mono nanofluid
(Asadi et al., 2018)	ϕ = 0.0125–0.015; T = 25–50 °C	Newtonian behavior

Table 3 Specifications of nanoparticles.

Nanoparticles	MWCNT	TiO_2
Purity	> 95 wt% (carbon nanotubes) (from TGA & TEM) > 97 wt% (carbon content)	99.9 + %
Outside diameter	5–15 nm (from HRTEM, Raman)	–
Inside diameter	3–5 nm	–
Length	50 um (TEM)	–
SSA	233 m^2/g (BET)	~ 35–60 m^2/g
Color	Black	white
Tap density	0.27 g/cm^3	0.25 g/cm^3
True density	~2.1 g/cm^3	4.23 g/cm^3

$$d = \frac{C\lambda}{B\cos\theta} \tag{2}$$

where λ is the wavelength with 1.5406 Å, B is the highest peak (FWHM), θ is Bragg angle and C is the crystal factor (0.9 ~ 1). Analysis of XRD curve peaks and using the Debye-Scherrer equation showed that most of the TiO_2 nanoparticle sizes are 40.08, 33.52, and 37.81 nm.

3. Results and discussion

3.1. Effect of parameters on μ_{nf}

If the shear stress varies nonlinear changes with the $\dot{\gamma}$, fluid has non-Newtonian behavior. One of the branches of non-Newtonian behavior is Pseudo-plastic behavior. Curve fitting of the experimental data has resulted in a model for nano lubricants behavior. So, curve fitting of the shear stress versus the $\dot{\gamma}$results in the power-law Ostwald de Waele (Andersson et al., 1992) that can predict the nano-lubricant behavior (Eq. (3)).

$$\tau_{yx} = m\left(\dot{\gamma}_{yx}\right)^n \tag{3}$$

μ_{nf} is in the form of Eq. (4) based on power-law (or Ostwald de Waele):

$$\mu_{nf} = \frac{\tau}{\dot{\gamma}} = m(\dot{\gamma})^{n-1} \tag{4}$$

In Eq.4, m and n are determined experimentally by curve fitting of the shear stress versus the $\dot{\gamma}$and are consistency index and power-law index, respectively. In this equation, when n < 1, fluid has pseudo-plastic characteristics (shear-thinning). For n = 1, fluid is Newtonian behavior and about n > 1, fluid's behavior is dilatant (shear-thickening) and as n value is lower, the order of pseudo-plasticity is higher. The most time-independent behavior in non-Newtonian fluids belongs to the pseudo-plastic (shear-thinning) behavior, which is identified by decreasing $\mu_{nf}$with the $\dot{\gamma}$. Fig. 2 shows a power-law index of nano-lubricants against the temperature at φ. Considering this figure, since the power-law index is less than unity in all temperatures and φ, nano-lubricants are non-Newtonian and of pseudo-plastic type. Also, with temperature enhancement of nano lubricant, the non-Newtonian behavior will continue. Fig. 3a shows the μ_{nf}versus the temperature. Temperature increase causes a drop-in resistance of nano-lubricant versus the exerted forces and the μ_{nf} decline of nano-lubricant. Results reveal that the μ_{nf} growth by 76 % with a shoot in the temperature at $\dot{\gamma}$ = 3999 s^{-1} and φ = 1 %. Increment of nanoparticles to the base fluid causes the formation and growth of nanoclusters, these nanoclusters prohibit the sliding of fluid layers on each other and increase the μ_{nf}. Fig. 3b shows μ_{nf} versus φ. It is apparent that the effect of nanoparticle addition on the enhancement of the μ_{nf} is lower at higher temperatures. It is necessary to mention that, because of the economic aspects like the cost of MWCNT and TiO_2,

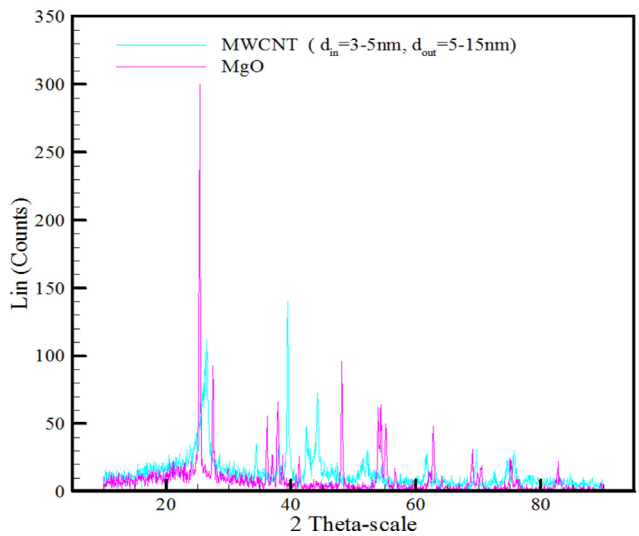

Fig. 1 X-ray diffraction pattern images of nanoparticles.

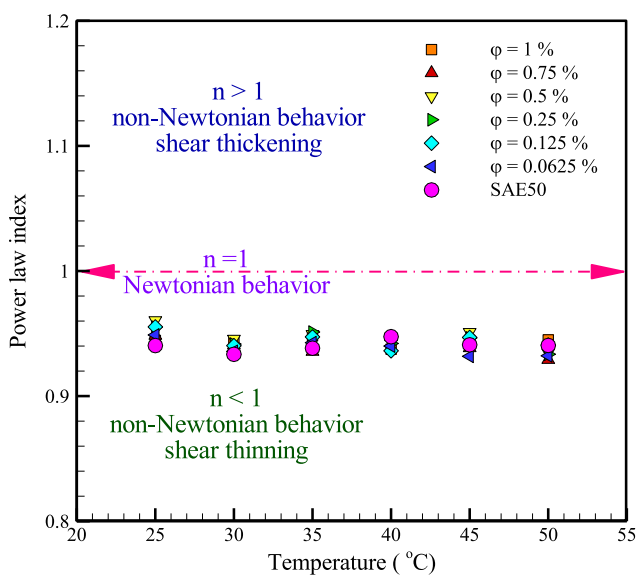

Fig. 2 Power-law index in terms of φ and temperatures.

and the evaluation of φ at low values (up to 1 %), φ is used in low values. Since most of the researchers investigated the thermophysical properties of nanofluids at φ = 1 to 5 %, evaluating the μ_{nf} and the behavior of nanofluids in the presence of low amounts of nanoparticles can be expressed as another novelty of the present study.

Fig. 4 shows the viscosity enhancement percent of MWCNT-TiO_2 (30:70)/SAE50 hybrid nano-lubricant versus φ at various temperatures. In low φ, a decrease in the μ_{nf} and in φ > 0.5 %, has created an increase in the μ_{nf}. Fig. 4 shows the maximum μ_{nf} reduction (-18 %) that was observed at T = 40 ℃ and φ = 0.0625 %. By increasing the number of nanoparticles in the base fluid, the number of collisions between particles and base fluid molecules noticeably goes up and this avoids sliding of fluid layers on each other which results in shoot up the μ_{nf}. Maximum μ_{nf} increase (+11 %) occurs at T = 25 ℃ and φ = 1 %. So, if we need a fluid with a lower μ_{nf}, it is better to use nano-lubricant with low φ.

3.2. Simulation of μ_{nf} with RSM

Choosing a model for the prediction of nano-lubricant properties can reduce the cost of repeating experiments. RSM evaluates suitable operational conditions using experimental data. RSM is a method for optimization of processes by mathematical and statistical correlations and can be used when different inputs affect the measurement and evaluation of a process (Bezerra et al., 2008). Different methods are used to evaluate the accuracy of a linear regression model (Wang et al., 2021), like least-squares estimation. In this investigation, Design of experiment software was used to model the viscosity of nanofluid. In this model, if n > k is assumed, it can be seen that variable answers will be available. It can be said $(y_1, y_2, \cdots, y_n)$. Along with each observed response y_i, we will have an observation on each regressor variable, let x_{ij} denote the observation or level of variable x_j. The matrix notation of the observations may be written as $y = X\beta + \varepsilon$, where X is the levels of the independent variables, β, is the regression coefficients, and ε is random errors. An unbiased estimator of parameters in multiple linear regression models is generated using the least-squares method. The summation of squares of residuals is a vital parameter and is calculated from Eq.5,

$$SS_E = \sum_{i=1}^{n} (y_i - \widehat{y}_i)^2 = \sum_{i=1}^{n} e_i^2 = e^T e \tag{5}$$

There are n × 1 vector of residuals, obtained from the difference of considerations (y_i) and fitted values $(\widehat{y}_i)$ that is denoted by:

$$e_i = y_i - \widehat{y}_i \tag{6}$$

Since $X^T Xb = X^T y$ the formula for computing SS_E may be shown as:

$$SS_E = y^T y - b^T X^T y \tag{7}$$

Eq.7 is known as error or residual sum of squares.

$$S_T = y^T y - \frac{\left(\sum_{i=1}^{n} y_i\right)^2}{n} = \sum_{i=1}^{n} y_i^2 - \frac{\left(\sum_{i=1}^{n} y_i\right)^2}{n} \tag{8}$$

Eq.8 is presented for the calculation of the total sum of squares. The determination coefficient (R^2) is calculated by Eq.9 (Palta et al., 1982);

$$R^2 = 1 - \frac{SS_E}{SS_T} \tag{9}$$

Evaluation of Eq. (9) shows that R^2 values are in the range of 0 to 1; if its value is close to 1, the accuracy of the model is higher. In some studies, R^2_{adj} is also investigated and is calculated from Eq.10 (Palta et al., 1982);

$$R^2_{adj} = 1 - \frac{SS_E/n-p}{SS_T/n-1} = 1 - \frac{n-1}{n-p}\left(1 - R^2\right) \tag{10}$$

where p is the regression coefficient and n is the number of measurements. R^2_{adj} will be decreased by adding too much of the parameter. As the parameters are added, the accuracy of the correlation will be decreased. Some of these parameters

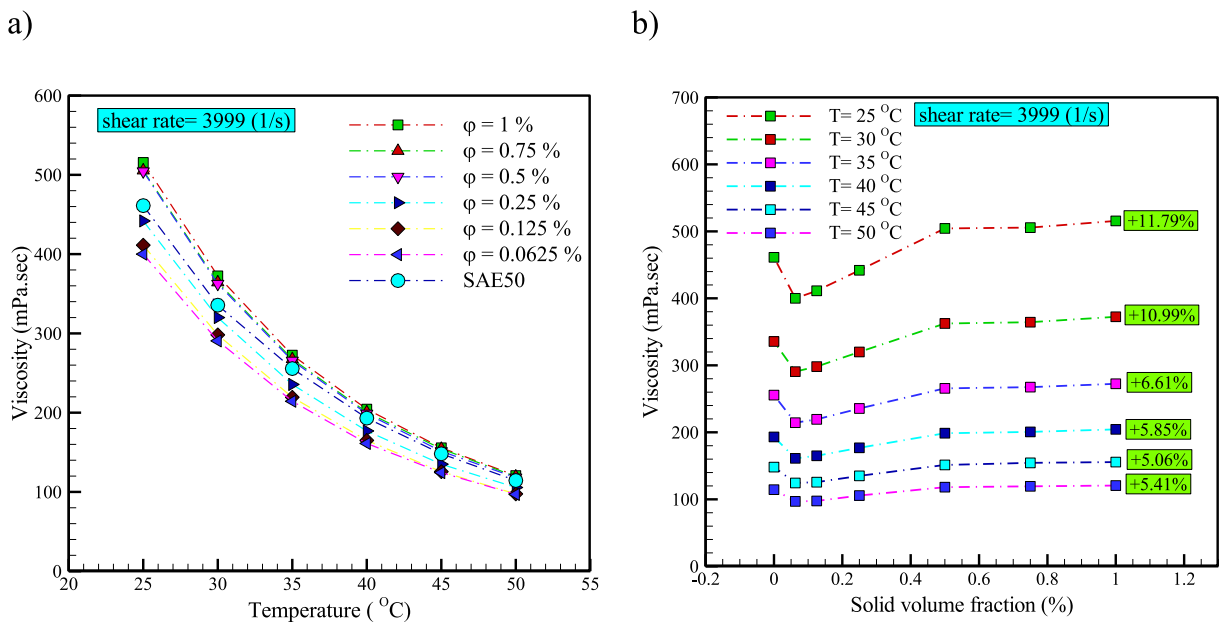

Fig. 3 **a)** μ_{nf} versus temperature. **b)** μ_{nf} versus at different φ.

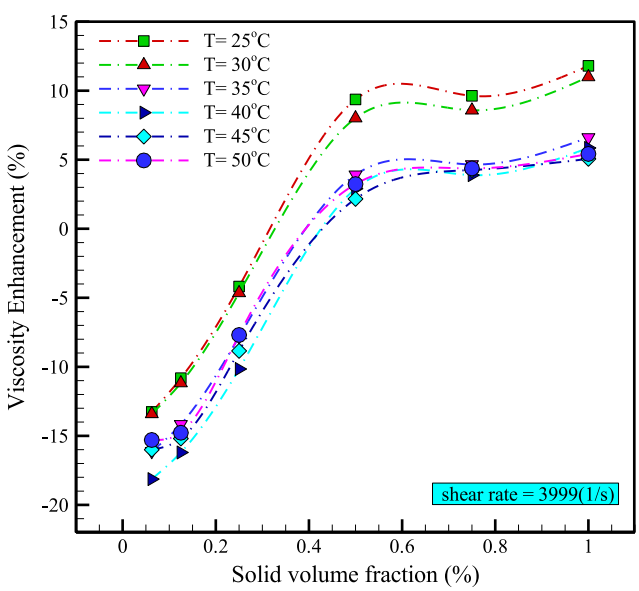

Fig. 4 Viscosity Enhancement versus φ at different temperatures.

are not important, and R^2_{adj} can recognize and remove them. This is the best way of adding unnecessary variables to the model without changing R^2 (Simpson et al., 1998). ANOVA method was employed to analyze the used model (Table 4) and prove its validity.

RSM was used to estimate the μ_{nf} in various temperatures, φ and $\dot{\gamma}$. Modeling with RSM results in Eq.11 for μ_{nf} based on φ, temperature, and $\dot{\gamma}$. Based on the p-value, it was decided which terms are included in the category of important sentences and which terms are excluded in the correlation equation. The criterion (critical) value for p-value is 0.05 and the terms of the equation that have a p-value > 0.05 are of little importance and can be removed.

$$\mu_{nf} = 1901.53 + 731.13\varphi - 97.42T - 0.042\dot{\gamma} - 20.28\varphi T + 0.0013T\dot{\gamma} - 302.39\varphi^2 + 1.83T^2 + 4.79\varphi^2 T + 0.14\varphi T^2 - 1.51 \times 10^{-5}T^2 - 0.012 \quad (11)$$

The proposed model can predict the μ_{nf} of MWCNT (30 %)-TiO_2 (70 %)/SAE50 hybrid nano-lubricant at φ = 0.0625 to 1 %, T = 25 to 50 ℃ and $\dot{\gamma}$ =666.5 and 7998 s^{-1}. The importance of the regression model can be figured out from the high F-value of 9888.233. P-values can determine statistical aspects of the model, when the p-value is < 0.05, that parameter is significant but parameters with p-values higher than 0.05 are less significant. So, non-significant parts of the model will be omitted. R^2 adj. of used model for the μ_{nf} is 0.999. It should be noted that R^2 adj. shows the quality of the output. As its value be closer to unity, the proposed model has higher accuracy. After correlating μ_{nf} with RSM, the conformism of predicted data with experimental data and residual values were checked to evaluate the quality of the model, and the results are presented in Fig. 5. Good conformity and low values of residuals (-12, +9) imply the high accuracy of the proposed model.

Three-dimensional μ_{nf} diagram against the $\dot{\gamma}$and temperature in $\dot{\gamma}$ = 6710.03 s^{-1} and versus temperature and $\dot{\gamma}$at φ = 0.51 % are depicted in Fig. 6. Fig. 6 shows that in low temperatures and $\dot{\gamma}$and high φ, the μ_{nf}has a higher value.

Fig. 7 presents the effects of each parameter on the μ_{nf}. It shows that the temperature has the maximum effect and $\dot{\gamma}$ quality of the output. As its value be closerhas minimum effect on the μ_{nf}. Also, the temperature and $\dot{\gamma}$ have opposite effects but φ has a direct effect on the μ_{nf}.

A computer with RAM 4.00 GB & CPU core i5 was used. The CPU time to reach the results at different μ_{nf} ($\dot{\gamma}$ = 5332 s^{-1}, T = 35 °C) was reported in Table 5. The infor-

Table 4 ANOVA for..μ_{nf}.

Source	Sum of Squares	df	Mean Square	F Value	p-value Prob > F
Model	2,757,867	19	145150.9	9888.233	< 0.0001
A-φ	7269.028	1	7269.028	495.1939	< 0.0001
B-T	74072.14	1	74072.14	5046.076	< 0.0001
C-$\dot{\gamma}$	322.2865	1	322.2865	21.95538	< 0.0001
AB	3110.403	1	3110.403	211.8925	< 0.0001
AC	14.11681	1	14.11681	0.961691	0.3283
BC	199.1713	1	199.1713	13.56831	0.0003
A^2	4474.296	1	4474.296	304.8061	< 0.0001
B^2	9574.162	1	9574.162	652.2284	< 0.0001
C^2	10.49573	1	10.49573	0.715009	0.3991
ABC	31.60646	1	31.60646	2.153153	0.1443
A^2B	1584.072	1	1584.072	107.913	< 0.0001
A^2C	1.27553	1	1.27553	0.086894	0.7686
AB^2	1135.7	1	1135.7	77.36822	< 0.0001
AC^2	7.81384	1	7.81384	0.532309	0.4667
B^2C	185.7014	1	185.7014	12.65068	0.0005
BC^2	0.072301	1	0.072301	0.004925	0.9441
A^3	22.43328	1	22.43328	1.528241	0.2183
B^3	2794.823	1	2794.823	190.394	< 0.0001
C^3	81.60985	1	81.60985	5.559574	0.0196
Residual	2260.59	154	14.67916		
Cor Total	2,760,128	173			

Standard deviation = 3.8313

R^2 (Adequate) = 0.9991, R^2 (Predicted) = 0.9989, R^2 (Adjusted) = 0.999

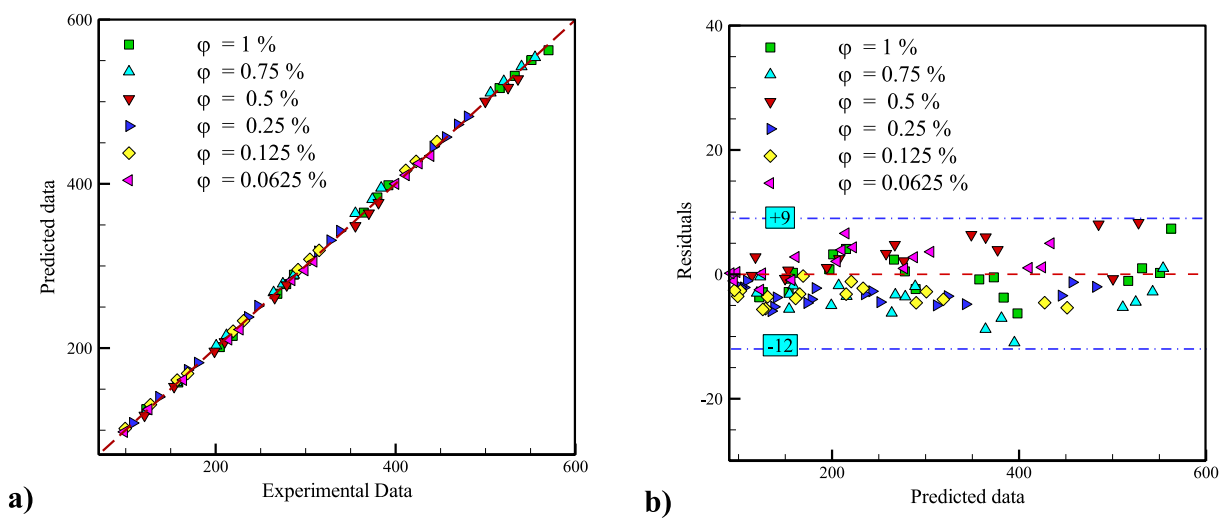

Fig. 5 **a)** Conformity of proposed model with experimental data **b)** Residuals versus predicted results.

mation in Table 5 is based on the information extracted from the design of experiment software and refers to the CPU time required to study the input data of the software based on the historical data method.

4. Simulation of μ_{nf} with ANN

In a complex information structure, in which the forecast utilizing ordinary techniques is lumbering and testing, the ANN gives a superior choice. The ANN can gain proficiency with very perplexing non-linear designed information. ANN is a computational model which learns like a human mind through epitomes. There are two main features that engineers have to face within natural processes. In the first step, they depend on many variables, in the second step, very complicated relations exist between the parts, so their analysis is so hard. This problem always affects the modeling accuracy. In this research, ANN was chosen between different modeling methods. Its main idea was adopted from the ANN of the human brain. The clearest likeness between a neural network and the brain

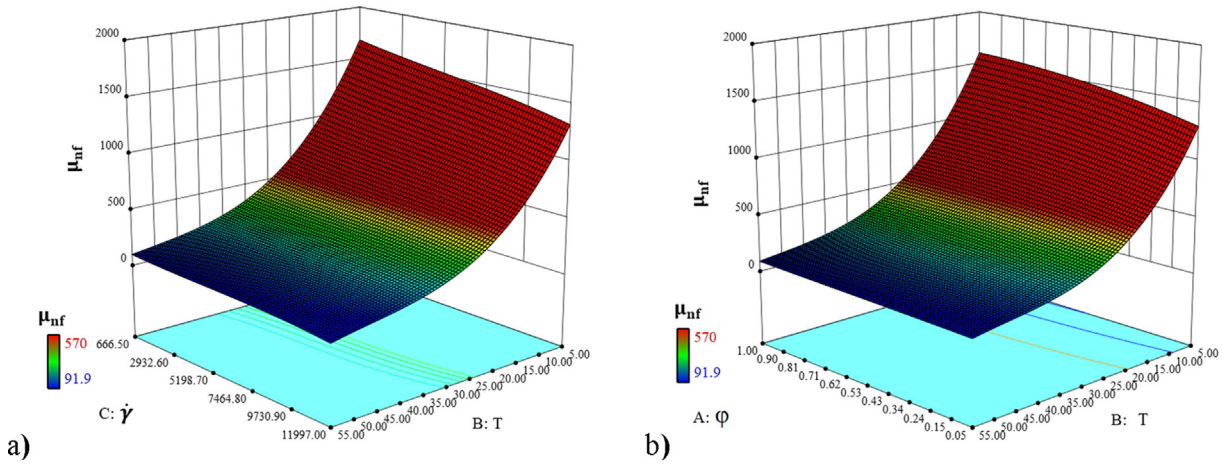

Fig. 6 3-Dimensional curves of **a)** μ_{nf} versus temperature and $\dot{\gamma}$ **b)** μ_{nf} versus temperature and φ.

is the presence of neurons as the most essential unit of the nervous system. However, how neurons take input in the two cases is unique. The creation of new structures for processing systems is the key parameter of this idea. To clarify process parameters, many data exist in this system that is called neurons that connect continuously. Synapse (electrochemical communication) is used for data transfer to coordinate them with each other. These ANNs can learn, and learning is a comparative concept for them. In other words, the weight of the synapse will be changed by using these samples and the system will give correct results in several ways including increasing hidden layers, changing activation function, changing activation function in the output layer, increasing the number of neurons, weight initialization, more data, and normalizing/scaling data (Behrang et al., 2010; Pedro and Maas, 2005; Yilmaz and Kaynar, 2011). Dropout is a regularization method that avoids overfitting the neural network. During training, it randomly releases neurons from the neural network, which is equivalent to training different neural networks. Different networks will excel differently, so the net effect of the regularization method will be to reduce redundant connections so that our model will be good for predictive analytics (Santos and Papa, 2022). The conventional method of solving Multilayer Perceptron (MLP) is the ANN. Two transfer functions that are used in the hidden layer and output layer are *tangent sigmoid* and *logistic sigmoid*. The levenberg-Marquardt algorithm was used for the determination of a suitable ANN structure. This algorithm changes the weight of neurons between real and target output, based on error. Several hidden layers are chosen depending on the complication level of the problem. First, the number of hidden layers is determined, and then in the next step, the number of neurons in hidden layers in the trial and error method is different to get the target output of the functions. This trend continues to find the number of neurons that result in a minimum error; this value will be reported as the optimum number of neurons in the hidden layer. There are several methods for determining the correct number of neurons to use in hidden layers:

- Between the size of the input layer and the size of the output layer.
- Two-thirds of the size of the input layer plus the size of the output layer.
- Less than twice the size of the input layer (Yu and Yan, 2019).

The output of multilayer perceptron **ANN** is mentioned below:

$$\gamma_{jk} = F_k\left(\sum_{i=1}^{N_{k-1}} w_{ijk}\gamma_{i(k-1)} + \beta_{jk}\right) \tag{12}$$

where γ_{jk} and β_{jk} are the output of j neuron from k layer and weight for j neuron in k layer. Parameters of compatibility model, w_{ijk} are the weights and were chosen randomly at the beginning of training. F_k is an active nonlinear activation transfer function that might be in different forms of identity function, binary step function, and binary sigmoid, bipolar sigmoid, Gaussian, and linear functions (Karlik and Olgac, 2011). In this paper, different activation functions of neurons were tested and then *logistic sigmoid* (Eq. (13)) and *tangent sigmoid* (Eq. (14)) functions were chosen for hidden and output layers,

$$f(\mathrm{x}) = \frac{1}{(1+e^{-x})} \tag{13}$$

$$f(\mathrm{x}) = \left[\frac{2}{1+e^{-2x}}\right] - 1 \tag{14}$$

100 structures of ANN with two hidden layers, each one containing 1 to 5 neurons and *tangent sigmoid* transfer function and *logistic sigmoid* transfer function were designed for each layer in this modeling. To determine the optimum structure for ANN, the fourth item in Table 6 which has two hidden layers with five and two neurons and *logistic sigmoid* transfer function for the first layer and *tangent sigmoid* transfer function for the second layer were chosen to consider calculated error values. Since the values of errors for this item were acceptable (MSE = 0.7663 and MAE = 1.3367) and R was close to unity (0.999957), some neurons were suitable too. The structure of the designed ANN is presented in Fig. 8.

The accuracy of the proposed structure was calculated from the below equations:

$$MSE = \frac{1}{N}\sum_{i=1}^{n}\left(T_{ij} - P_{ij}\right)^2 \tag{15}$$

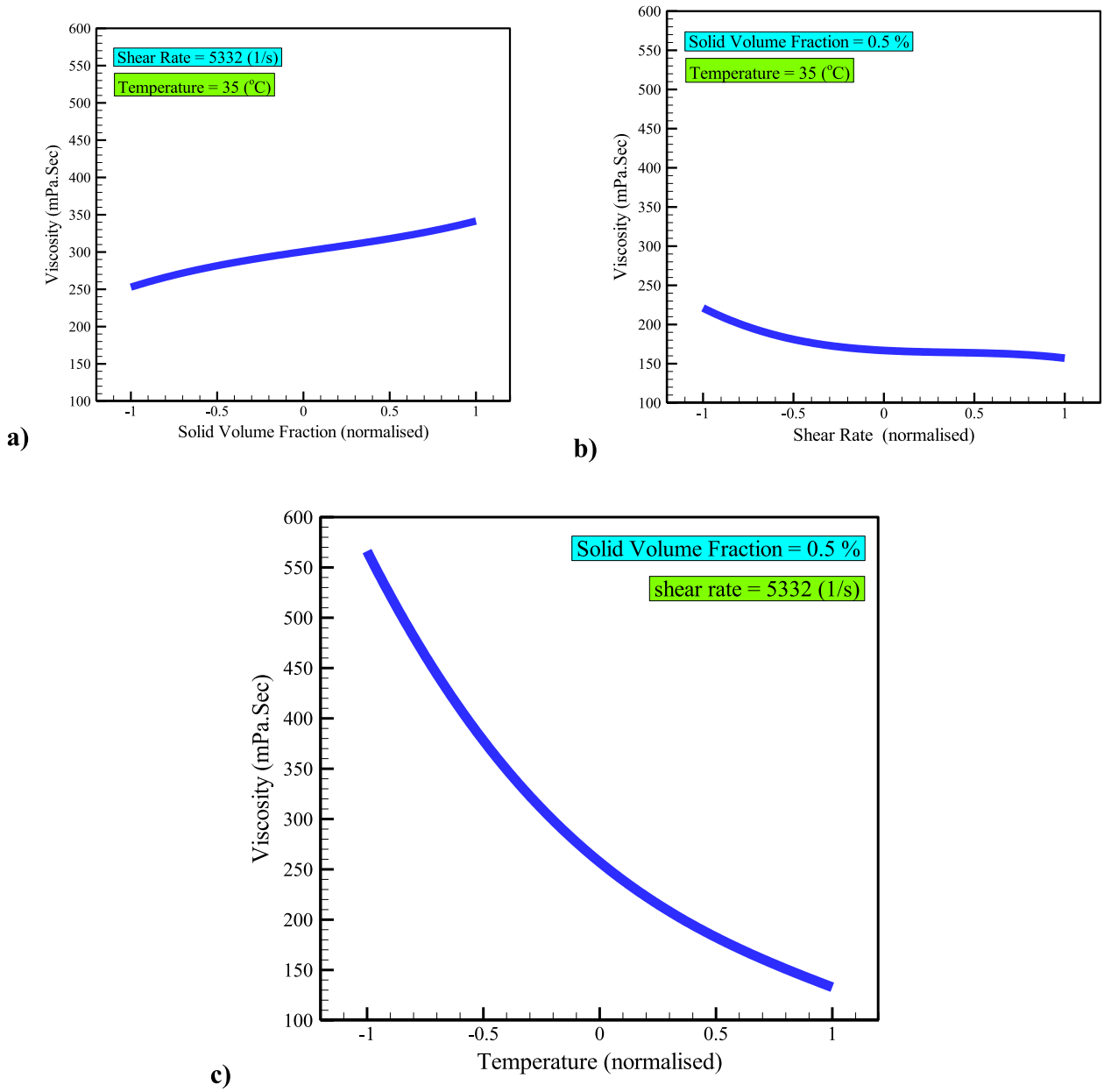

Fig. 7 Effect of **a)** solid volume fraction **b)** shear rate **c)** temperature parameter on..μ_{nf}

Table 5 CPU Time for different..μ_{nf}.

μ_{nf}	260.22	275.36	286.44	290.55
CPU time (second)	4.10	5.25	6.11	7.08

$$MAE = \frac{1}{N}\sum_{i=1}^{n}\left(T_{ij} - P_{ij}\right) \tag{16}$$

$$R = \frac{\sum_{i=1}^{n}\left(T_{ij} - \bar{T}\right)\left(P_{ij} - \bar{p}\right)}{\sqrt{\sum_{i=1}^{n}\left(T_{ij} - \bar{T}\right)^2 \sum_{i=1}^{n}\left(P_{ij} - \bar{p}\right)^2}} \tag{17}$$

$$R^2 = \frac{\sum_{i=1}^{n}\left(T_{ij} - \bar{T}\right)^2 - \sum_{i=1}^{n}\left(P_{ij} - \bar{p}\right)^2}{\sum_{i=1}^{n}\left(T_{ij} - \bar{\bar{T}}\right)^2} \tag{18}$$

$$MAPE = \frac{1}{n}\sum_{i=1}^{n}\left|\frac{\left(P_{ij} - T_{ij}\right)}{T_{ij}}\right| \times 100 \tag{19}$$

Table 6 Optimum structures of ANN.

ROW	Structure	Transfer Function	R	R^2	MAPE	RSME	MAE	MSE
1	[3 1]	*logistic tangent*	0.999897	0.9998	0.4320	1.3751	1.1874	3.2805
2	[3 2]	*logistic tangent*	0.999930	0.9999	0.4316	1.3742	0.9202	2.2391
3	[4 4]	*tangent logistic*	0.999943	0.9999	0.4322	1.3769	0.838	1.8289
4	**[5 2]**	***logistic tangent***	**0.999957**	**0.9999**	**0.4322**	**1.3761**	**0.7663**	**1.3367**

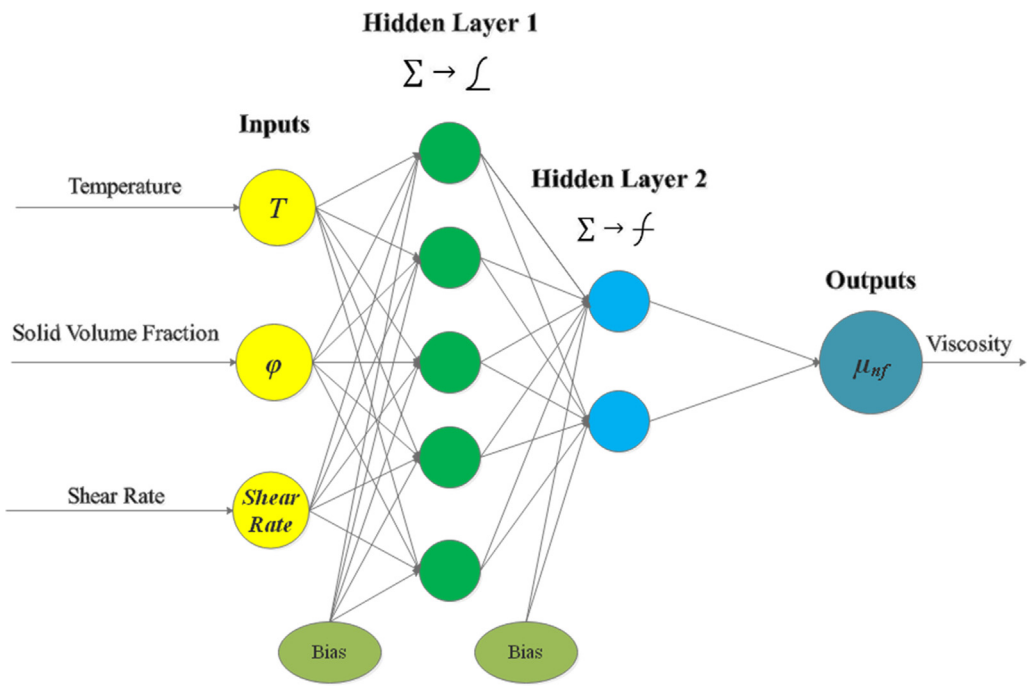

Fig. 8 Topology of a typical **ANN** structure.

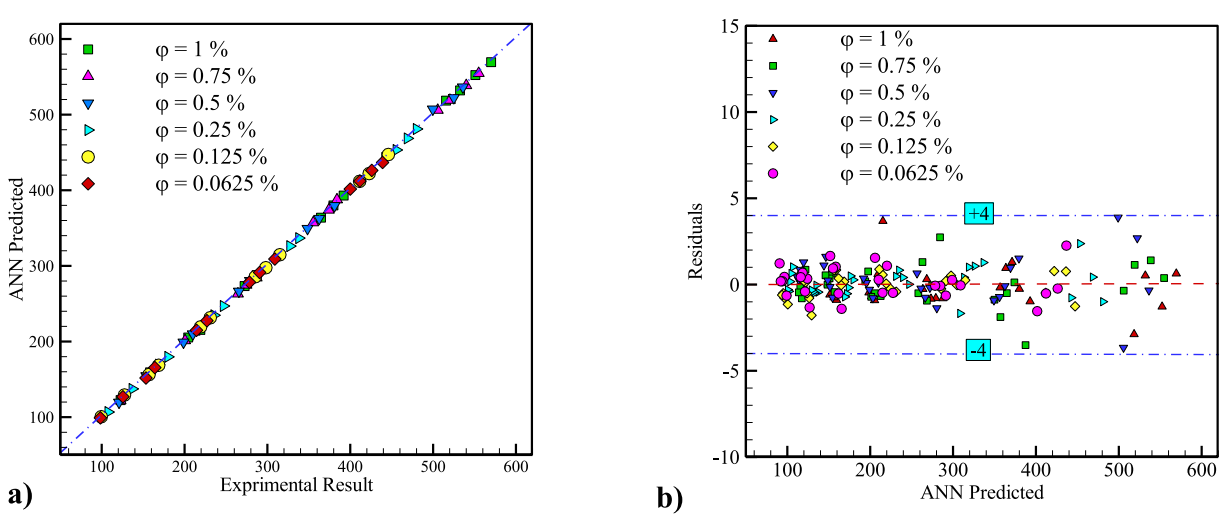

Fig. 9 **a)** Curve of compliance between **ANN** data with experimental data **b)** Residuals **ANN** results.

$$RSME = \sqrt{\frac{1}{n}\sum_{i=1}^{n}\left(P_{ij} - T_{ij}\right)^2} \tag{20}$$

In the above equations, T_{ij} is the experimental value and P_{ij} is the estimated value from the model. $\bar{T}$ and $\bar{p}$ are the mean experimental values and values estimated by the model for n data.

As Fig. 9 shows, all data are spread around the oblique line. Minimum and maximum differences between values of experimental data and predicted data by the ANN method were ± 4 %. Analysis shows that the proposed ANN model is a valid and exact model for the prediction of μ_{nf}.

Fig. 10 shows an analogy among the empirical data and predicted results by training, test, validation, and all data of ANN. According to this figure, predicted results by ANN could properly cover the experimental data. This shows that ANN was trained properly which resulted in an acceptable accuracy of the test, validation, and all data.

5. Comparison of ANN model with RSM

In this part, a comparison is done between the presented model by RSM (Eq. (11)) and the ANN method to reach the best model. As it is evident in Fig. 11, both models could predict empirical data with good approximation in different φ and temperatures.

Fig. 12 shows the margin of deviation for the proposed model by RSM (Eq. (11)) and ANN method at different φ. The margin of deviation is calculated from Eq. (21),

$$MOD(\%) = \frac{100}{N}\sum_{i=1}^{N}\left|\frac{\mu_{nf}|_{Pred} - \mu_{nf}|_{Exp}}{\mu_{nf}|_{Exp}}\right| \tag{21}$$

As it is obvious, **ANN** has the least value of MOD (%) in all φ. Based on the results obtained from graphs 5 and 9 mentioned above. So, it results that the ANN model can estimate the experimental data more accurately with less error.

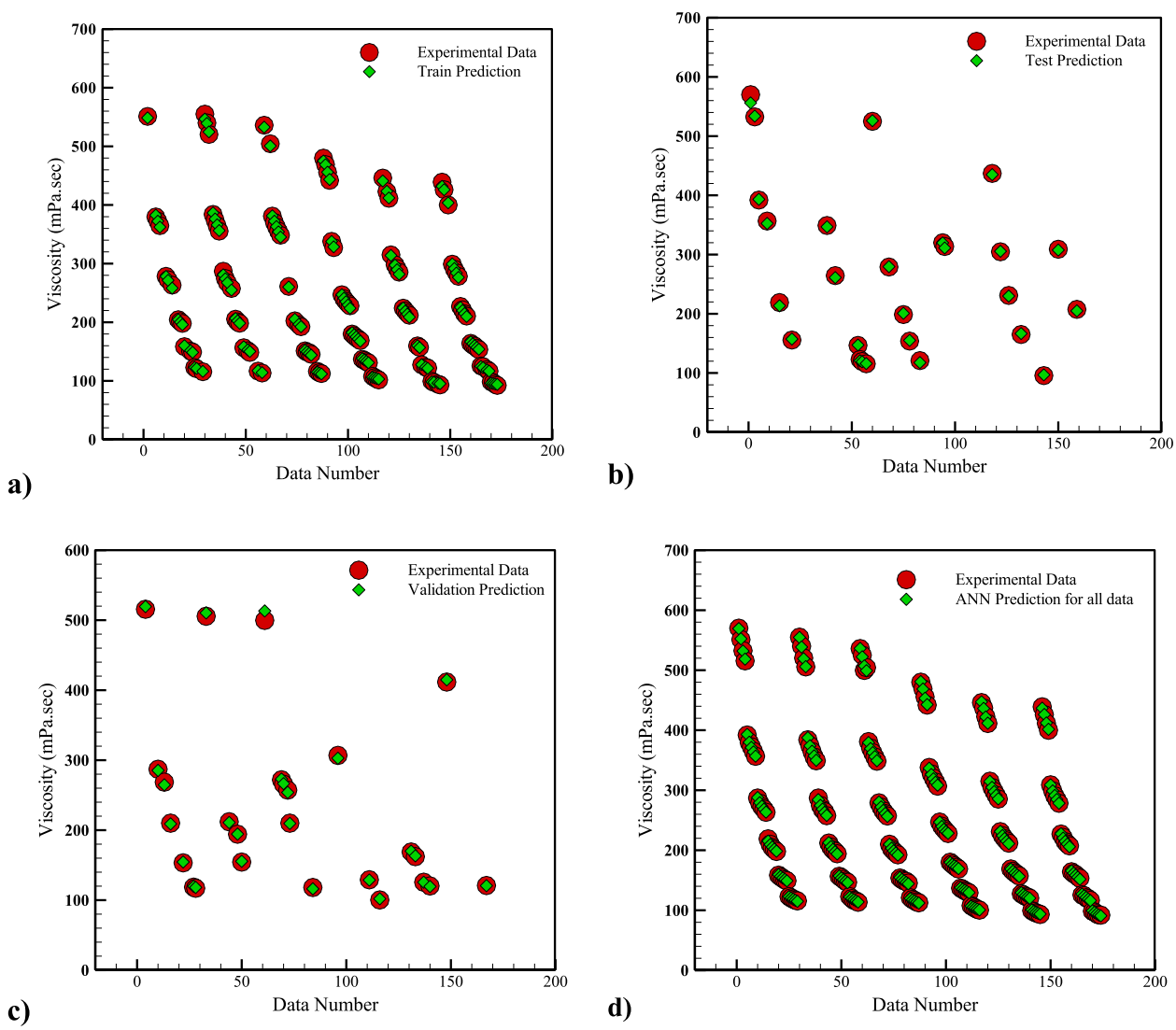

Fig. 10 ANN Prediction performance on **a)** training **b)** test **c)** validation **d)** all data.

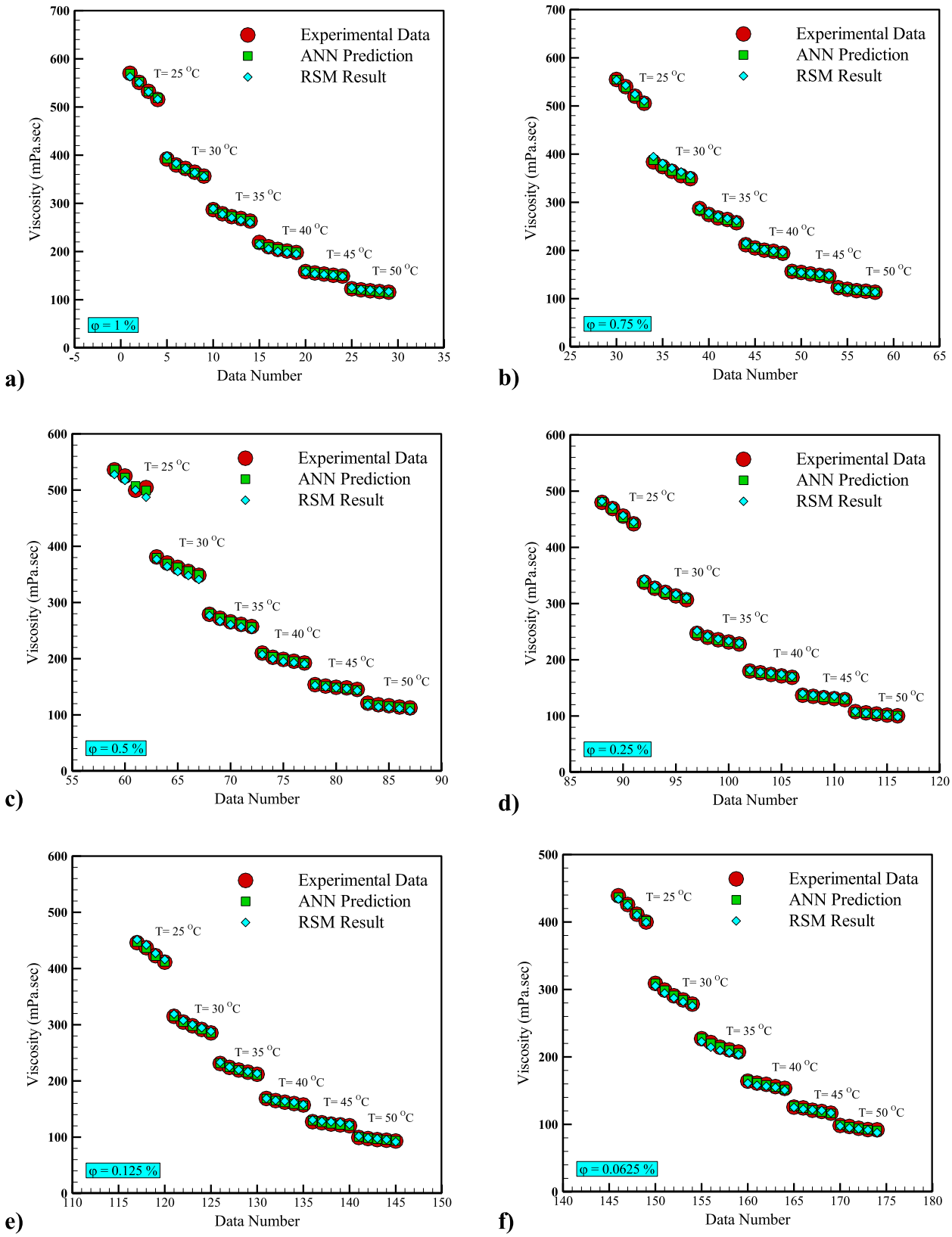

Fig. 11 Comparison of **ANN** prediction with the **RSM** result using experimental data for **a)** φ = 1 % **b)** φ = 0.75 % **c)** φ = 0.5 % **d)** φ = 0.25 % **e)** φ = 0.125 % **f)** φ = 0.0625 %.

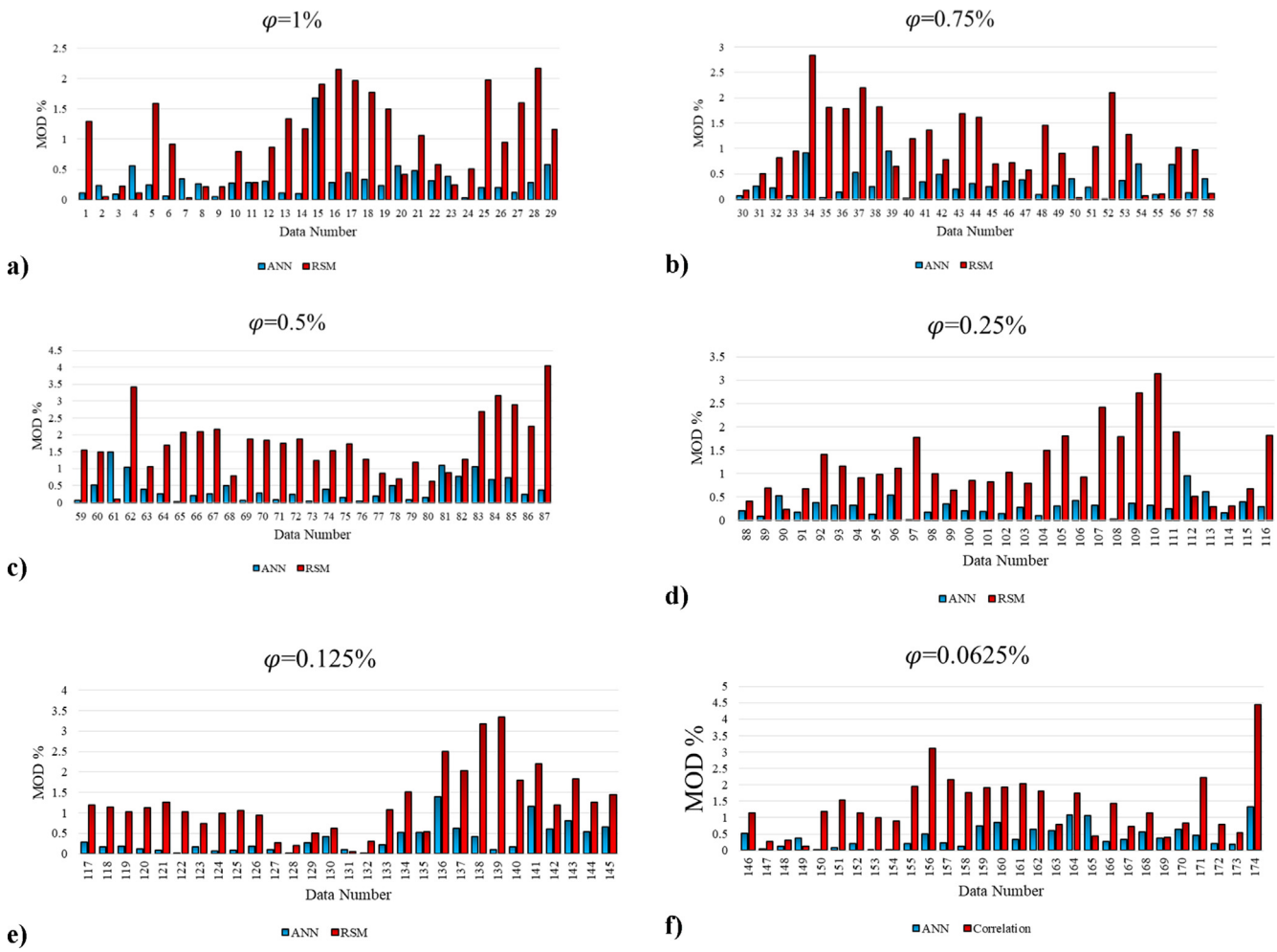

Fig. 12 Comparison of error for **ANN** and **RSM** model in **a)** φ = 1 % **b)** φ = 0.75 % **c)** φ = 0.5 % **d)** φ = 0.25 % **e)** φ = 0.125 % **f)** φ = 0.0625 %.

6. Conclusion

In this paper, experimental data obtained for μ_{nf} of MWCNT (30 %)-TiO_2 (70 %)/SAE50 hybrid nano-lubricant were modeled using RSM and ANN methods. By comparing the accuracy parameters for ANN and RSM models, it was concluded that the proposed ANN model predicts the empirical data more accurately. Statistical regression analysis of training and test data (R^2 = 0.9999), Mean Square Error (MSE) = 1.3367 and Mean Absolute Error (MAE = 0.7663) have shown the ability of improved ANN in the prediction of μ_{nf}. The following results were also obtained:

- Since the power-law index is less than one at all temperatures and φ, nano-lubricants are non-Newtonian and pseudo-plastic (shear-thinning).
- R^2 in the proposed model by RSM method for prediction of μ_{nf} was 0.9991 which shows the high accuracy of the correlation.
- Analysis reveals that temperature and $\dot{\gamma}$ have the maximum and minimum effects on μ_{nf}, respectively.
- Maximum and minimum difference between experimental and predicted data by ANN was ± 4 % which shows the acceptable correctness of the model.
- Comparison of MOD of two presented models revealed that MOD of **ANN** has a lower value at all φ. This implies that ANN is more accurate in the prediction of μ_{nf}.

Declaration of Competing Interest

The authors declare that they have no known competing financial interests or personal relationships that could have appeared to influence the work reported in this paper.

References

Abbasian Arani, A.A., Amani, J., Hemmat Esfeh, M., 2012. Numerical simulation of mixed convection flows in a square double lid-driven cavity partially heated using nanofluid. J. Nanostruct. 2 (3), 301–311.

Abbasian Arani, A.A., Kakoli, E., Hajialigol, N., 2014. Double-diffusive natural convection of Al2O3-water nanofluid in an enclosure with partially active side walls using variable properties. J. Mech. Sci. Technol. 28 (11), 4681–4691.

Abbasian Arani, A.A., Abbaszadeh, M., Ardeshiri, A., 2016. Mixed convection fluid flow and heat transfer and optimal distribution of discrete heat sources location in a cavity filled with nanofluid. Transp. Phenom. Nano Micro Scales 5 (1), 30–43.

Abbasian Arani, A.A., Sadripour, S., Kermani, S., 2017. Nanoparticle shape effects on thermal-hydraulic performance of boehmite alumina nanofluids in a sinusoidal–wavy mini-channel with phase shift and variable wavelength. Int. J. Mech. Sci. 128, 550–563.

Abdul Hamid, K., Azmi, W.H., Nabil, M.F., Mamat, R., Sharma, K. V., 2018. Experimental investigation of thermal conductivity and dynamic viscosity on nanoparticle mixture ratios of TiO2-SiO2 nanofluids. Int. J. Heat Mass Transfer 116, 1143–1152.

Abu-Hamdeh, N.H., Golmohammadzadeh, A., Karimipour, A., 2021. Performing regression-based methods on viscosity of nano-enhanced PCM-Using ANN and RSM. J. Mater. Res. Technol. 10, 1184–1194.

Aghaei, A., Khorasanizadeh, H., Sheikhzadeh, G.A., 2018. Measurement of the dynamic viscosity of hybrid engine oil-Cuo-MWCNT nanofluid, development of a practical viscosity correlation and utilizing the artificial neural network. Heat Mass Transfer 54 (1), 151–161.

Aghahadi, M.H., Niknejadi, M., Toghraie, D., 2019. An experimental study on the rheological behavior of hybrid Tungsten oxide (WO3)-MWCNTs/engine oil Newtonian nanofluid. J. Mol. Struct. 1197, 497–507.

Ahmadi, M.H., Ahmadi, M.A., Alhuyi Nazari, M., Mahian, O., Ghasempour, R., 2019. A proposed model to predict thermal conductivity ratio of Al2O3/EG nanofluid by applying least squares support vector machine (LSSVM) and genetic algorithm as a connectionist approach. J. Therm. Anal. Calorimetry 135 (1), 271–281.

Ahmadi, M.H., Mohseni-Gharyehsafa, B., Farzaneh-Gord, M., Jilte, R.D., Kumar, R., Chau, K.W., 2019. Applicability of connectionist methods to predict dynamic viscosity of silver/water nanofluid by using ANN-MLP, MARS and MPR algorithms. Eng. Appl. Comput. Fluid Mech. 13 (1), 220–228.

Alarifi, I.M., Alkouh, A.B., Vakkar, A., Nguyen, H.M., Asadi, A., 2019. On the rheological properties of MWCNT-TiO2/oil hybrid nanofluid: an experimental investigation on the effects of shear rate, temperature, and solid concentration of nanoparticles. Powder Technol. 355, 157–162.

Alirezaie, A., Saedodin, S., Hemmat Esfe, M., Rostamian, S.H., 2016. Investigation of rheological behavior of MWCNT (COOH functionalized)/MgO - Engine oil hybrid nanofluids and modelling the results with artificial neural networks. J. Mol. Liq. 241, 173–181.

Alirezaie, A., Saedodin, S., Esfe, M.H., Rostamian, S.H., 2017. Investigation of rheological behavior of MWCNT (COOH-functionalized)/MgO-engine oil hybrid nanofluids and modelling the results with artificial neural networks. J. Mol. Liq. 241, 173–181.

Alirezaie, A., Hajmohammad, M.H., Ahangar, M.R.H., Hemmat Esfe, M., 2018. Price-performance evaluation of thermal conductivity enhancement of nanofluids with different particle sizes. Appl. Therm. Eng. 128, 373–380.

Andersson, H.I., Bech, K.H., Dandapat, B.S., 1992. Magnetohydrodynamic flow of a power-law fluid over a stretching sheet. Int. J. Non-Linear Mech. 27 (6), 929–936.

Asadi, A., Asadi, M., Rezaee, M., Siahmargoi, F., 2016. The effect of temperature and solid concentration on dynamic viscosity of MWCNT/MgO (20–80)–SAE50 hybrid nano-lubricant and proposing a new correlation: an experimental study. Int. Commun. Heat Mass Transfer 78, 48–53.

Asadi, M., Asadi, A., 2016. Dynamic viscosity of MWCNT/ZnO–engine oil hybrid nanofluid: an experimental investigation and new correlation in different temperatures and solid concentrations. Int. Commun. Heat Mass Transfer 76, 41–45.

Asadi, M., Asadi, A., Aberoumand, S., 2018. An experimental and theoretical investigation on the effects of adding hybrid nanoparticles on heat transfer efficiency and pumping power of an oil-based nanofluid as a coolant fluid. Int. J. Refrig. 89, 83–92.

Asadi, A., Asadi, M., Rezaniakolaei, A., Rosendahl, L.A., Afrand, M., Wongwises, S., 2018. Heat transfer efficiency of Al2O3-MWCNT/thermal oil hybrid nanofluid as a cooling fluid in thermal and energy management applications: an experimental and theoretical investigation. Int. J. Heat Mass Transfer 117, 474–486.

Asif, Muhammad Adnan. "A Theoretical Study of the Size Effect of Carbon Nanotubes on the Removal of Water Chemical Contaminants." Journal of Research in Science, Engineering and Technology 6, no. 04 (2018): 21-27. DOI: https://doi.org/10.24200/jrset.vol6iss04pp21-27.

Athab, A., Lafta, A.J., Hussein, F.H., 2015. Modification of carbon nanotubes surface using different oxidizing agents. J. Environ. Anal. Chem 2, e112.

Azin, Z., Pourghobadi, Z., 2021. Electrochemical sensor based on nanocomposite of multi-walled carbon nano-tubes (MWCNTs)/TiO_2/carbon ionic liquid electrode analysis of acetaminophen in pharmaceutical formulations. Iran. J. Chem. Chem. Eng. (IJCCE) 40 (4), 1030–1041. https://doi.org/10.30492/ijcce.2020.39811.

Behrang, M.A., Assareh, E., Ghanbarzadeh, A., Noghrehabadi, A. R., 2010. The potential of different artificial neural network (ANN) techniques in daily global solar radiation modeling based on meteorological data. Solar Energy 84 (8), 1468–1480.

Bezerra, M.A., Santelli, R.E., Oliveira, E.P., Villar, L.S., Escaleira, L. A., 2008. Response surface methodology (RSM) as a tool for optimization in analytical chemistry. Talanta 76 (5), 965–977.

Chu, Y.M., Ibrahim, M., Saeed, T., Berrouk, A.S., Algehyne, E.A., Kalbasi, R., 2021. Examining rheological behavior of MWCNT-TiO2/5W40 hybrid nanofluid based on experiments and RSM/ANN modeling. J. Mol. Liq. 333, 115969.

Dastmalchi, M., Sheikhzadeh, G.A., Abbasian Arani, A.A., 2015. Double-diffusive natural convective in a porous square enclosure filled with nanofluid. Int. J. Therm. Sci. 95, 88–98.

Desai, H.B., Kumar, A., Tanna, A.R., 2021. Structural and magnetic properties of MgFe2O4 ferrite na-noparticles synthesis through auto combustion technique. Eur. Chem. Bull. 10 (3), 186–190.

Doust, A.M., Rahimi, M., Feyzi, M., 2015. Effects of solvent addition and ultrasound waves on viscosity reduction of residue fuel oil. Chem. Eng. Process.: Process Intensif. 95, 353–361.

Dwijendra, N.K.A., Patra, I., Ahmed, Y.M., et al, 2022. Carbonyl sulfide gas detection by pure, Zn- and Cd-decorated AlP nanosheet. Monatsh Chem. https://doi.org/10.1007/s00706-022-02961-5.

Esfe, M.H., Motallebi, S.M., 2019. Four objective optimization of aluminum nanoparticles/oil, focusing on thermo-physical properties optimization. Powder Technol. 356, 832–846.

Esfe, M.H., Motallebi, S.M., 2021. Viscosity modeling of nano-modified SAE50 engine oil using RSM and ANN methods. Int. Commun. Heat Mass Transfer 128, 105542.

Esfe, M.H., Wongwises, S., Naderi, A., Asadi, A., Safaei, M.R., Rostamian, H., Karimipour, A., 2015. Thermal conductivity of Cu/TiO2–water/EG hybrid nanofluid: experimental data and modeling using artificial neural network and correlation. Int. Commun. Heat Mass Transfer 66, 100–104.

Esfe, M.H., Arani, A.A.A., Rezaie, M., Yan, W.M., Karimipour, A., 2015. Experimental determination of thermal conductivity and dynamic viscosity of Ag–MgO/water hybrid nanofluid. Int. Commun. Heat Mass Transfer 66, 189–195.

Esfe, M.H., Yan, W.M., Akbari, M., Karimipour, A., Hassani, M., 2015. Experimental study on thermal conductivity of DWCNT-ZnO/water-EG nanofluids. Int. Commun. Heat Mass Transfer 68, 248–251.

Esfe, M.H., Ahangar, M.R.H., Rejvani, M., Toghraie, D., Hajmohammad, M.H., 2016. Designing an artificial neural network to predict dynamic viscosity of aqueous nanofluid of TiO 2 using experimental data. Int. Commun. Heat Mass Transfer 75, 192–196.

Esfe, M.H., Amiri, M.K., Alirezaie, A., 2018. Thermal conductivity of a hybrid nanofluid. J. Therm. Anal. Calorimetry 134 (2), 1113–1122.

Esfe, M.H., Rostamian, H., Rejvani, M., Emami, M.R.S., 2018. Rheological behavior characteristics of ZrO2-MWCNT/10W40 hybrid nano-lubricant affected by temperature, concentration, and shear rate: an experimental study and a neural network simulating. Phys. E: Low-dimensional Syst. Nanostruct. 102, 160–170.

Esfe, M.H., Kamyab, M.H., Afrand, M., Amiri, M.K., 2018. Using artificial neural network for investigating of concurrent effects of multi-walled carbon nanotubes and alumina nanoparticles on the viscosity of 10W–40 engine oil. Phys. A: Statist. Mech. Appl. 510, 610–624.

Esfe, M.H., Arani, A.A.A., Esfandeh, S., 2018. Improving engine oil lubrication in light-duty vehicles by using of dispersing MWCNT and ZnO nanoparticles in 5W50 as viscosity index improvers (VII). Appl. Therm. Eng. 143, 493–506.

Esfe, M.H., Raki, H.R., Emami, M.R.S., Afrand, M., 2019. Viscosity and rheological properties of antifreeze based nanofluid containing hybrid nano-powders of MWCNTs and TiO2 under different temperature conditions. Powder Technol. 342, 808–816.

Esfe, M.H., Emami, M.R.S., Amiri, M.K., 2019. Experimental investigation of effective parameters on MWCNT–TiO 2/SAE50 hybrid nanofluid viscosity. J. Therm. Anal. Calorimetry 137 (3), 743–757.

Esfe, M.H., Esfandeh, S., Amiri, M.K., Afrand, M., 2019. A novel applicable experimental study on the thermal behavior of SWCNTs (60%)-MgO (40%)/EG hybrid nanofluid by focusing on the thermal conductivity. Powder Technol. 342, 998–1007.

Esfe, M.H., Amiri, M.K., Bahiraei, M., 2019. Optimizing thermophysical properties of nanofluids using response surface methodology and particle swarm optimization in a non-dominated sorting genetic algorithm. J. Taiwan Inst. Chem. Eng. 103, 7–19.

Esfe, M.H., Abad, A.T.K., Fouladi, M., 2019. Effect of suspending optimized ratio of nano-additives MWCNT-Al2O3 on viscosity behavior of 5W50. J. Mol. Liq. 285, 572–585.

Esfe, M.H., Hajian, M., Esmaily, R., Eftekhari, S.A., Hekmatifar, M., Toghraie, D., 2022. Designing the best ANN topology for predicting the dynamic viscosity and rheological behavior of MWCNT-CuO (30: 70)/SAE 50 nano-lubricant. Colloids Surf. A: Physicochem. Eng. Asp. 651, 129691.

Esfe, Mohammad Hemmat; Saedodin, Seyfolah; Biglari, Mojtaba; Rostamian, Hadi; ,Experimental investigation of thermal conductivity of CNTs-Al2O3/water: a statistical approach,International Communications in Heat and Mass Transfer,69,,29-33,2015, Pergamon.

Esfe, Mohammad Hemmat; Hajmohammad, Mohammad Hadi; , Thermal conductivity and viscosity optimization of nanodiamond-Co3O4/EG (40: 60) aqueous nanofluid using NSGA-II coupled with RSM,Journal of Molecular Liquids,238,,545-552,2017, Elsevier.

Esfe, Mohammad Hemmat; Rostamian, Hossein; Sarlak, Mohammad Reza; Rejvani, Mousa; Alirezaie, Ali; ,"Rheological behavior characteristics of TiO2-MWCNT/10w40 hybrid nano-oil affected by temperature, concentration and shear rate: an experimental study and a neural network simulating",Physica E: Low-dimensional Systems and Nanostructures,94,,231-240,2017,North-Holland.

Gao, T., Li, C., Zhang, Y., Yang, M., Jia, D., Jin, T., Hou, Y., Li, R., 2019. Dispersing mechanism and tribological performance of vegetable oil-based CNT nanofluids with different surfactants. Tribol. Int. 131, 51–63. https://doi.org/10.1016/j.triboint.2018.10.025.

R. Gharibshahi, A. Jafari M. Omidkhah, J.R. Nezhad, Performance experimental investigation of novel multifunctional nanohybrids on enhanced oil recovery. AIP Conference Proceedings. Vol. 1920(1) (2018) AIP Publishing.

Ghasemi, S., Karimipourm, A., 2018. Experimental investigation of the effects of temperature and mass fraction on the dynamic viscosity of CuO-paraffin nanofluid. Appl. Therm. Eng. 128, 189–197.

Gholami, E., Vaferi, B., Ariana, M.A., 2018. Prediction of viscosity of several alumina-based nanofluids using various artificial intelligence paradigms-comparison with experimental data and empirical correlations. Powder Technol. 323, 495–506.

Ghorabaee, H., Emami, M.R.S., Shafahi, M., 2019. Effect of nanofluid and surfactant on thermosyphon heat pipe performance. Heat Transfer Eng., 1–14

Gulzar, O., Qayoum, A., Gupta, R., 2019. Experimental study on stability and rheological behaviour of hybrid Al2O3-TiO2 therminol-55 nanofluids for concentrating solar collectors. Powder Technol. 352, 436–444.

Gupta, S., 2022. Magnetic nanoparticles supported sulfuric acid as a green and efficient nanocatalyst for oxidation of sulfides and oxidative coupling of thiols. J. Synth. Chem. 1 (1), 16–21. https://doi.org/10.22034/jsc.2022.149217.

Hemmat, M., Davoodi, A., 2019. Power-efficient ReRAM-aware CNN model generation. Integration 69, 369–380.

Hemmat Esfe, M., 2018. The investigation of effects of temperature and nanoparticles volume fraction on the viscosity of copper oxide-ethylene glycol nanofluids. Period. Polytech. Chem. Eng. 62 (1), 43.

M. Hemmat Esfe, A.A. Abbasian Arani, An experimental determination and accurate prediction of dynamic viscosity of MWCNT (% 40)-SiO2 (% 60)/5W50 nano-lubricant, J. Molecular Liquids 259 (2018) 227-237.

Hemmat Esfe, M., Saedodin, S., Asadi, A., Karimipour, A., 2015. Thermal conductivity and viscosity of Mg(OH)2-ethylene glycol nanofluids. J. Therm. Anal. Calorimetry 120 (2), 1145–1149.

Hemmat Esfe, M., Saedodin, S., Biglari, M., Rostamian, H., 2016. An experimental study on thermophysical properties and heat transfer characteristics of low volume concentrations of Ag-water nanofluid. Int. Commun. Heat Mass Transfer 74, 91–97.

Hemmat Esfe, M., Hajmohammad, H., Moradi, R., Abbasian Arani, A.A., 2017. Multi-objective optimization of cost and thermal performance of double walled carbon nanotubes/water nanofluids by NSGA-II using response surface method. Appl. Therm. Eng. 112, 1648–1657.

Hemmat Esfe, M., Hajmohammad, H., Toghraie, D., Rostamian, H., Mahian, O., Wongwises, S., 2017. Multi-objective optimization of nanofluid flow in double tube heat exchangers for applications in energy systems. Energy 137, 160–171.

Hemmat Esfe, M., Tilebon, S.M.S., 2019. Statistical and artificial based optimization on thermo-physical properties of an oil based hybrid nanofluid using NSGA-II and RSM. Physica A. https://doi.org/10.1016/j.physa.2019.122126.

Hemmat Esfe, M., Razi, P., Hajmohammad, M.H., Rostamian, S.H., Sarsam, W.S., Abbasian Arani, A.A., Dahari, M., 2017. Optimization, modeling and accurate prediction of thermal conductivity and dynamic viscosity of stabilized ethylene glycol and water mixture Al2O3 nanofluids by NSGA-II using ANN. Int. Commun. Heat Mass Transfer 82, 154–160.

Hemmat Esfe, M., Rostamian, H., Shabani-samghabadi, A., Abbasian Arani, A.A., 2017. Application of three-level general factorial design approach for thermal conductivity of MgO/water nanofluids. Appl. Therm. Eng. 127, 1194–1199.

Hemmat Esfe, M., Rejvani, M., Karimpour, R., Abbasian Arani, A. A., 2017. Estimation of thermal conductivity of ethylene glycol-based nanofluid with hybrid suspensions of SWCNT-Al2O3 nanoparticles by correlation and ANN methods using experimental data. J. Therm. Anal. Calorimetry 128 (3), 1359–1371.

Hemmat Esfe, M., Alirezaie, A., Rejvani, M., 2017. An applicable study on the thermal conductivity of SWCNT-MgO hybrid nanofluid and price-performance analysis for energy management. Appl. Therm. Eng. 111, 1202–1210.

Hemmat Esfe, M., Abbasian Arani, A.A., Aghaie, A., Wongwises, S., 2017. Mixed convection flow and heat transfer in an up-driven, inclined, square enclosure subjected to DWCNT-water nanofluid containing three circular heat sources. Curr. Nanosci. 13 (3), 311–323.

Hemmat Esfe, M., Karimpour, R., Abbasian Arani, A.A., Shahram, J., 2017. Experimental investigation on non-Newtonian behavior of Al2O3-MWCNT/5W50 hybrid nano-lubricant affected by alter-

ations of temperature, concentration and shear rate for engine applications. Int. Commun. Heat Mass Transfer 82, 97–102.
Hemmat Esfe, M., Behbahani, P.M., Abbasian Arani, A.A., Sarlak, M.R., 2017. Thermal conductivity enhancement of SiO2–MWCNT (85: 15%)–EG hybrid nanofluids. J. Therm. Anal. Calorimetry 128 (1), 249–258.
Hemmat Esfe, M., Abbasian Arani, A.A., Madadi, M.R., Alirezaie, A., 2018. A study on rheological characteristics of hybrid nano-lubricants containing MWCNT-TiO2 nanoparticles. J. Mol. Liq. 260, 229–236.
Hemmat Esfe, M., Esfandeh, S., 2018. Investigation of rheological behavior of hybrid oil based nanolubricant-coolant applied in car engines and cooling equipments. Appl. Therm. Eng. 131, 1026–1033.
Hemmat Esfe, M., Saedodin, S., Rejvani, M., Shahram, J., 2017. Experimental investigation, model development and sensitivity analysis of rheological behavior of ZnO/10W40 nano-lubricants for automotive applications. Phys. E: Low-dimensional Syst. Nanostruct. 90, 194–203.
Hemmat Esfe, M., Tatar, A., Ahangar, M.R.H., Rostamian, H., 2017. A comparison of performance of several artificial intelligence methods for predicting the dynamic viscosity of TiO2/SAE 50 nano-lubricant. Physica E: Low-dimensional Syst. Nanostruct. 96, 85–93.
Hemmat Esfe, M., Zabihi, F., Rostamian, H., Esfandeh, S., 2017. Experimental investigation, model development of the non-Newtonian behavior of CuO-MWCNT-10w40 nano-lubricant for lubrication purposes. J. Mol. Liq. 249, 677–687.
Hemmat Esfe, M., Wongwises, S., Esfandeh, S., Alirezaie, A., 2018. Development of a new correlation and post processing of heat transfer coefficient and pressure drop of functionalized COOH MWCNT nanofluid by artificial neural network. Curr. Nanosci. 14 (2), 104–112.
Hemmat Esfe, M., Bahiraei, M., Mahian, O., 2018. Experimental study for developing an accurate model to predict viscosity of CuO–ethylene glycol nanofluid using genetic algorithm based neural network. Powder Technol. 338, 383–390.
Hemmat Esfe, M., Abbasian Arani, A.A., Esfandeh, S., 2018. Experimental study on rheological behavior of monograde heavy-duty engine oil containing CNTs and oxide nanoparticles with focus on viscosity analysis. J. Mol. Liq. 272, 319–329.
Hemmat Esfe, M., Esfandeh, S., Afrand, M., Rejvani, M., Rostamian, S.H., 2018. Experimental evaluation, new correlation proposing and ANN modeling of thermal properties of EG based hybrid nanofluid containing ZnO-DWCNT nanoparticles for internal combustion engines applications. Appl. Therm. Eng. 133, 452–463.
Hemmat Esfe, M., Amiri, M.K., Alirezaie, A., 2018. Thermal conductivity of a hybrid nanofluid. J. Therm. Anal. Calorimetry 134 (2), 1113–1122.
Hemmati-Sarapardeh, A., Varamesh, A., Husein, M.M., Karan, K., 2018. On the evaluation of the viscosity of nanofluid systems: modeling and data assessment. Renew. Sustain. Energy Rev. 81, 313–329.
Holzwarth, U., Gibson, N., 2011. The Scherrer equation versus the'Debye-Scherrer equation. Nat. Nanotechnol. 6 (9), 534.
Huai, Z., Wang, H., Gong, M., 2021. Research on keeping the formation for multiple aircrafts based on deep convolutional neural networks[J]. J. Ordnance Equip. Eng. 42 (02), 15–22.
Izadi, F., Ranjbarzadeh, R., Kalbasi, R., Afrand, M., 2018. A new experimental correlation for non-Newtonian behavior of COOH-DWCNTs/antifreeze nanofluid. Phys. E: Low-dimensional Syst. Nanostruct. 98, 83–89.
Karlik, B., Olgac, A.V., 2011. Performance analysis of various activation functions in generalized MLP architectures of neural networks. Int. J. Artif. Intell. Expert Syst. 1 (4), 111–122.
Kazemi, M., Shiri, L., 2022. Ionic liquid immobilized on magnetic nanoparticles: a nice and efficient catalytic strategy in synthesis of heterocycles. J. Synth. Chem. 1 (1), 1–7. https://doi.org/10.22034/jsc.2022.149201.
Kherbeet, A.S., Mohammed, H.A., Salman, B.H., Ahmed, H.E., Alawi, O.A., Rashidi, M.M., 2015. Experimental study of nanofluid flow and heat transfer over microscale backward-and forward-facing steps. Exp. Therm. Fluid Sci. 65, 13–21.
Lebon, G., Hatim, M., 2018. A thermodynamic model of nanofluid viscosity based on a generalized Maxwell-type constitutive equation. J. Non-Newtonian Fluid Mech. 253, 1–6.
Li, H., Zhao, R., 2022. Dissociation of ammonia borane and its subsequent nucleation on the Ru(0001) surface revealed by density functional theoretical simulations. Phys. Chem. Chem. Phys. https://doi.org/10.1039/D1CP05957B.
Liu, Y., Yin, D., Tian, M., Hu, X., Chen, X., 2018. Experimental investigation on the viscosity of hybrid nanofluids made of two kinds of nanoparticles mixed in engine oil. Micro & Nano Lett. 13 (8), 1197–1202.
Maddah, H., Aghayari, R., Ahmadi, M.H., Rahimzadeh, M., Ghasemi, N., 2018. Prediction and modeling of MWCNT/Carbon (60/40)/SAE 10 W 40/SAE 85 W 90 (50/50) nanofluid viscosity using artificial neural network (ANN) and self-organizing map (SOM). J. Therm. Anal. Calorimetry 134 (3), 2275–2286.
Mahian, O., Kolsi, L., Amani, M., Estellé, P., Ahmadi, G., Kleinstreuer, C., Marshall, J.S., Taylor, R.A., Abu-Nada, E., Rashidi, S., Niazmand, H., Wongwises, S., Hayat, T., Kasaeian, A., Pop, I., 2019. Recent advances in modeling and simulation of nanofluid flows—part II: applications. Phys. Rep. 791, 1–59.
Mahian, O., Kolsi, L., Amani, M., Estellé, P., Ahmadi, G., Kleinstreuer, K., Marshall, J.S., Siavashi, M., Taylor, R.A., Niazmand, H., Wongwises, S., Hayat, T., Kolanjiyil, A., Kasaeian, A., Pop, I., 2019. Recent advances in modeling and simulation of nanofluid flows-Part I: Fundamentals and theory. Phys. Rep. 790, 1–48.
Mansoury, D., Doshmanziari, F.I., Rezaie, S., Rashidi, M.M., 2019. Effect of Al 2 O 3/water nanofluid on performance of parallel flow heat exchangers. J. Therm. Anal. Calorimetry 135 (1), 625–643.
Mehrabi, M., Sharifpur, M., Meyer, J.P., 2013. Viscosity of nanofluids based on an artificial intelligence model. Int. Commun. Heat Mass Transfer 43, 16–21.
Mirsaeidi, A.M., Yousefi, F., 2021. Viscosity, thermal conductivity and density of carbon quantum dots nanofluids: an experimental investigation and development of new correlation function and ANN modeling. J. Therm. Anal. Calorimetry 143 (1), 351–361.
Mohammad Hosein Fakhar, Ahmad Fakhar and Hamidreza Tabatabaei, Nanotechnology efficacy on improvement of acute velocity in fluid-conveyed pipes under thermal load, International Journal of HydromechatronicsVol. 4, No. 2, pp 142-154https://doi.org/10.1504/IJHM.2021.116956.
Palta, M., Prineas, R.J., Berman, R., Hannan, P., 1982. Comparison of self-reported and measured height and weight. Am. J. Epidemiol. 115 (2), 223–230.
Pedro, J.C., Maas, S.A., 2005. A comparative overview of microwave and wireless power-amplifier behavioral modeling approaches. IEEE Trans. Microwave Theory Tech. 53 (4), 1150–1163.
Rakshe, S., Nimje, S.V., Panigrahi, S.K., 2021. Optimization of adhesively bonded Spar-Wingskin joints of laminated FRP composites subjected to pull-off load: a critical review. Rev. Adhes. Adhes. 8 (1), 29–46. https://doi.org/10.7569/RAA.2020.097303.
Rostamian, S.H., Biglari, M., Saedodin, S., Hemmat Esfe, M., 2017. An inspection of thermal conductivity of CuO-SWCNTs hybrid nanofluid versus temperature and concentration using experimental data, ANN modeling and new correlation. J. Mol. Liq. 231, 364–369.
Santos, C. F. G. D., & Papa, J. P. (2022). Avoiding overfitting: A survey on regularization methods for convolutional neural networks. ACM Computing Surveys (CSUR).
Ruhani, B. et al, 2019. Statistical investigation for developing a new model for rheological behavior of Silica–ethylene glycol/Water

hybrid Newtonian nanofluid using experimental data. Physica A 525, 616–627.

Ruhani, B. et al, 2019. Statistical investigation for developing a new model for rheological behavior of ZnO–Ag (50%–50%)/Water hybrid Newtonian nanofluid using experimental data. Physica A 525, 741–751.

Simpson, T.W., Mauery, T.M., Korte, J.J., Mistree, F., 1998. Comparison of response surface and kriging models for multidisciplinary design optimization. 7th AIAA/USAF/NASA/ISSMO Sympos. Multidiscip. Anal. Optimiz.

Tian, C., 2021. Calculation method of impact point parameter based on BP neural network for submarine launched ballistic missile. J. Ordnance Equip. Eng. 42 (04), 145–149.

Tian, S., Arshad, N.I., Toghraie, D., Eftekhari, S.A., Hekmatifar, M., 2021. Using perceptron feed-forward Artificial Neural Network (ANN) for predicting the thermal conductivity of graphene oxide-Al2O3/water-ethylene glycol hybrid nanofluid. Case Stud. Therm. Eng. 26, 101055.

Toghraie, D., Sina, N., Jolfaei, N.A., Hajian, M., Afrand, M., 2019. Designing an Artificial Neural Network (ANN) to predict the viscosity of Silver/Ethylene glycol nanofluid at different temperatures and volume fraction of nanoparticles. Phys. A: Statist. Mech. Appl. 534, 122142.

Wang, W., Lei, Y., Yan, T., Li, N., Nandi, A., 2021. Residual convolution long short-term memory network for machines remaining useful life prediction and uncertainty quantification. J. Dyn., Monit. Diagnos. 1 (1), 2–8. https://doi.org/10.37965/jdmd.v2i2.43.

Wang, Y., Li, C., Zhang, Y., Yang, M., Li, B., Jia, D., Hou, Y., Mao, C., 2016. Experimental evaluation of the lubrication properties of the wheel/workpiece interface in minimum quantity lubrication (MQL) grinding using different types of vegetable oils. J. Clean. Prod. 127, 487–499. https://doi.org/10.1016/j.jclepro.2016.03.121.

Wei, B., Zou, C., Yuan, X., Li, X., 2017. Thermo-physical property evaluation of diathermic oil based hybrid nanofluids for heat transfer applications. Int. J. Heat Mass Transfer 107, 281–287.

Yang, M., Li, C., Zhang, Y., Jia, D., Zhang, X., Hou, Y., Li, R., Wang, J., 2017. Maximum undeformed equivalent chip thickness for ductile-brittle transition of zirconia ceramics under different lubrication conditions. Int. J. Mach. Tools Manuf. 122, 55–65. https://doi.org/10.1016/j.ijmachtools.2017.06.003.

Yilmaz, I., Kaynar, O., 2011. Multiple regression, ANN (RBF, MLP) and ANFIS models for prediction of swell potential of clayey soils. Expert Syst. Appl. 38 (5), 5958–5966.

Yu, J., Yan, X., 2019. Whole process monitoring based on unstable neuron output information in hidden layers of deep belief network. IEEE Trans. Cybernetics 50 (9), 3998–4007.

Zaferani, S.P.G., Emami, M.R.S., Amiri, M.K., Binaeian, E., 2019. Optimization of the removal Pb (II) and its Gibbs free energy by thiosemicarbazide modified chitosan using RSM and ANN modeling. Int. J. Biol. Macromol. 139, 307–319.

Zhang, G., Chen, J., Zhang, Z., Sun, M., Yu, Y., Wang, J.,... Cai, S. (2022). Analysis of magnetorheological clutch with double cup-shaped gap excited by Halbach array based on finite element method and experiment. Smart Materials and Structures. doi: 10.1088/1361-665X/ac701a.

Zhang, Y., Li, C., Jia, D., Zhang, D., Zhang, X., 2015. Experimental evaluation of MoS2 nanoparticles in jet MQL grinding with different types of vegetable oil as base oil. J. Clean. Prod. 87, 930–940. https://doi.org/10.1016/j.jclepro.2014.10.027.

Zhang, Y., Li, C., Jia, D., Zhang, D., Zhang, X., 2015. Experimental evaluation of the lubrication performance of MoS2/CNT nanofluid for minimal quantity lubrication in Ni-based alloy grinding. Int. J. Mach. Tools Manuf. 99, 19–33. https://doi.org/10.1016/j.ijmachtools.2015.09.003.

Zhang, G., Zhang, Z., Sun, M., Yu, Y., Wang, J., Cai, S., 2022. The influence of the temperature on the dynamic behaviors of magnetorheological gel. Adv. Eng. Mater., 2101680 https://doi.org/10.1002/adem.202101680.

Further Reading

Esfe, M.H., Esfandeh, S., Arani, A.A.A., 2019. Proposing a modified engine oil to reduce cold engine start damages and increase safety in high temperature operating conditions. Powder Technol. 355, 251–263.

Esfe, M.H., Arani, A.A.A., Esfandeh, S., Afrand, M., 2019. Proposing new hybrid nano-engine oil for lubrication of internal combustion engines: preventing cold start engine damages and saving energy. Energy 170, 228–238.

Hemmat Esfe, M., Toghraie, D., 2021. An optimal feed-forward artificial neural network model and a new empirical correlation for prediction of the relative viscosity of Al2O3-engine oil nanofluid. Scient. Rep. 11 (1), 1–14.